



BACCHUS

Impact of Biogenic versus Anthropogenic emissions on Clouds and Climate: towards a Holistic UnderStanding

Collaborative Project

SEVENTH FRAMEWORK PROGRAMME

ENV.2013.6.1-2

Atmospheric processes, eco-systems and climate change

Grant agreement no: 603445

Deliverable number:	D3.2
Deliverable name:	Joint top-down and bottom-up CDNC/ICNC closure studies
WP number:	3
Delivery date:	Project month 24 (30/11/2015)
Actual date of submission:	30/11/2015
Dissemination level:	PU
Lead beneficiary:	UMAN
Responsible scientist/administrator:	Paul Connolly
Estimated effort (PM):	18
Contributor(s):	Paul Connolly, Matt Crooks (UMAN), Philip Stier, Laurent Labbouz (UOXF); Danny Rosenfeld, Eyal Hashimshoni (HUJI); Stefano Decesari (CNR-ISAC); Giulia Saponaro (FMI)
Estimated effort contributor(s) (PM):	80
Internal reviewer:	Philip Stier (UOXF)

Summary of results

In this task we combine traditional bottom-up cloud droplet / ice crystal number concentration (CDNC/ICNC) closure studies with a novel concept of top-down closures studies to provide constraints on the satellite inferred cloud microphysical properties concentrations and for validation of products used in Task 3.4. We have compared the effective radius retrieved from the VIIRS satellite with that from in-situ data. We have also modelled these cases to test closure at various different levels. Our finding is that effective radius is in reasonable agreement between satellite and in-situ data and that the bottom-up closure works well. However, we find that the cloud drop number concentration retrieved from satellite in shallow convection that is of maritime nature can be underestimated and that updraft velocities are a critical component in the subsequent retrieval of cloud condensation nuclei (CCN). We provide suggestions for how this underestimation may be overcome.

Background

This task combines traditional *bottom-up* CDNC closure studies with a novel concept of *top-down* closures studies.

Bottom-up: for the bottom-up closure studies we make use of data from WP1 to conduct parcel model closure studies of cloud microphysical parameters. We combine standard approaches with the detailed Aerosol-Cloud-Precipitation Interactions Model (ACPIM) cloud parcel model (UMAN) (Connolly et al., 2012; Topping et al., 2013) and optimal parameter estimation methods based on Markov Chain Monte Carlo (MCMC) parcel modelling (Partridge et al., 2012). In addition, we have evaluated the convective cloud field model (CCFM, Wagner & Graf, 2010) used in MPI-ESM in single column mode nudged by observed meteorology.

Top down: Based on the vertical profile of the dependence of the effective radius on cloud top temperature from the NPP/ Visible Infrared Imaging Radiometer Suite (NPP/VIIRS) imager (375 μm) data retrieved in WP1 and temperature the number of activated aerosol particles at cloud base, N_a , has been retrieved in non-precipitating convective clouds (Freud et al., 2011). This has been used to infer CCN concentrations from satellites in a manner similar to Rosenfeld et al. (2012).

Methodology

In order to retrieve droplet number concentrations in convective clouds, Rosenfeld et al. (2015) have applied NPP/VIIRS retrievals of effective radius and applied the assumption of an adiabatic cloud. The effective radius can be thought of as the ratio of the third to second moments of a size distribution:

$$r_{eff} = \frac{\int nr^3 dr}{\int nr^2 dr}$$

where r_{eff} is the effective radius, n is the drop number distribution and r is the drop radius.

With additional measurements of aerosol hygroscopicity and assumptions to estimate the cloud base updraft speed (e.g. Twomey, 1959), this novel approach is able to use clouds as CCN counters. The method works as follows. Firstly, effective radius is retrieved in the tops of growing cumulus cells. From knowledge of cloud base temperature and pressure a calculation of the adiabatic liquid water content is performed and this is set equal to the product of droplet number concentration and the average mass, determined from the effective radius as using:

$$\frac{4}{3}\pi\rho r_{eff}^3 N_d = LWC$$

where LWC is the liquid water content, N_d is the drop number concentration and ρ is the density of liquid water.

The number of cloud drops is then determined by solving for N_d , which yields

$$r_{eff} = \left(\frac{3LWC}{4\pi\rho} \right)^{1/3} \tag{1}$$

In this report we present an evaluation of this approach in shallow convection over the UK, with moderately cold cloud bases to heavily polluted deep convection over the Amazon.

In-situ data considered

Aircraft *in-situ* datasets considered to perform this analysis are shown in Figure 1¹. It was found that due to a combination of factors (whether there were satellite overpasses from NPP / VIIRS; and the requirement for good observations inside convective cells) that the suitable field projects were the COPE (UK) and SAMBBA (Brazil) field campaigns. GO-AMAZON (Brazil) is another dataset we wish to exploit; however, at the present time the data are not widely available. ICE-D is another field campaign we wish to exploit when VIIRS data become available for this recent project in the future.

¹ In addition we have considered ground-based data from the Po valley and Mace Head.

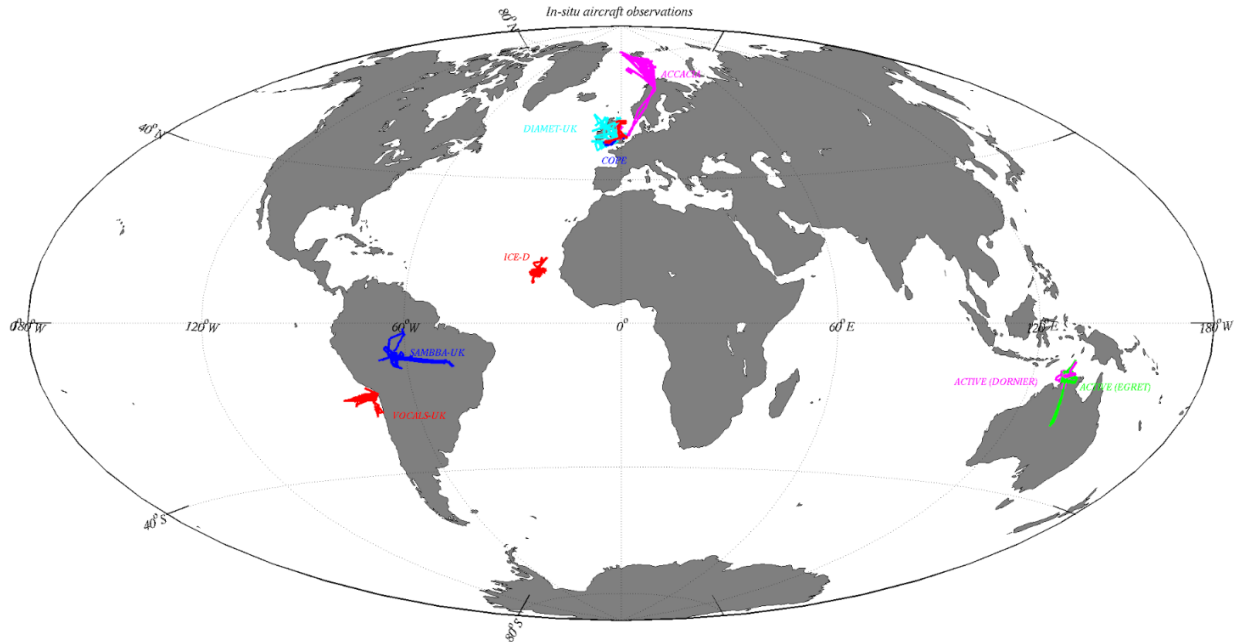


Figure 1. In-situ datasets considered for this deliverable. VOCALS was a stratocumulus project, SAMBBA sampled convective clouds over the Amazon; ICE-D sampled convection and the transition to hurricanes / impact of dust outbreaks; COPE studied shallow convection over the UK; ACTIVE and EMERALD-II studied deep convection over Darwin; ACCACIA studied Arctic stratus and DIAMET studied mesoscale storms.

Several cases were deemed suitable for analysis following an assessment of the satellite overpass times and flight times, etc (see Table 1.)

Table 1. Subset of cases deemed suitable for analysis. Acronyms (Cb=cumulonimbus, Cu=cumulus, Sc=stratocumulus, MCS=mesoscale convective system).

Project	Date	Description
SAMBBA	2012/09/14	Smoky environment (potentially other cases too)
COPE	2013/06/25	Shallow polluted convection
COPE	2013/07/25	Clean cumulus congestus
ICE-D	2015/07/22	Cumulus with layer clouds
ICE-D	2015/08/06	MCS deep convective clouds
ICE-D	2015/08/11	Sc to Cb transition
ICE-D	2015/08/21	Cb and layer clouds

GOAMAZON	2014/09/06	Convective, Cb
GOAMAZON	2014/09/11	Convective, Cb
GOAMAZON	2014/09/21	Polluted Cu
GOAMAZON	2014/09/27	Polluted Cu
GOAMAZON	2014/09/30	Sc
Po Valley	2012/06/14	Convective
Mace Head	2015/08/11	Thin clouds
Mace Head	2015/08/16	Convective clouds inland

Shallow cumulus / congestus case study

We now provide an example case study of shallow convection over the UK during the COPE field experiment in July 2013. Two cases were deemed suitable for analysis and are shown in Figure 2. The first is a case of shallow convection over East Anglia on the 25th June 2013 (Figure 2, left plot), whereas the second is a case of cumulus congestus over the Cornish peninsula on the 25th July 2013. (Figure 2, right plot). The second case is the one we focus on here as it highlights a number of key points.

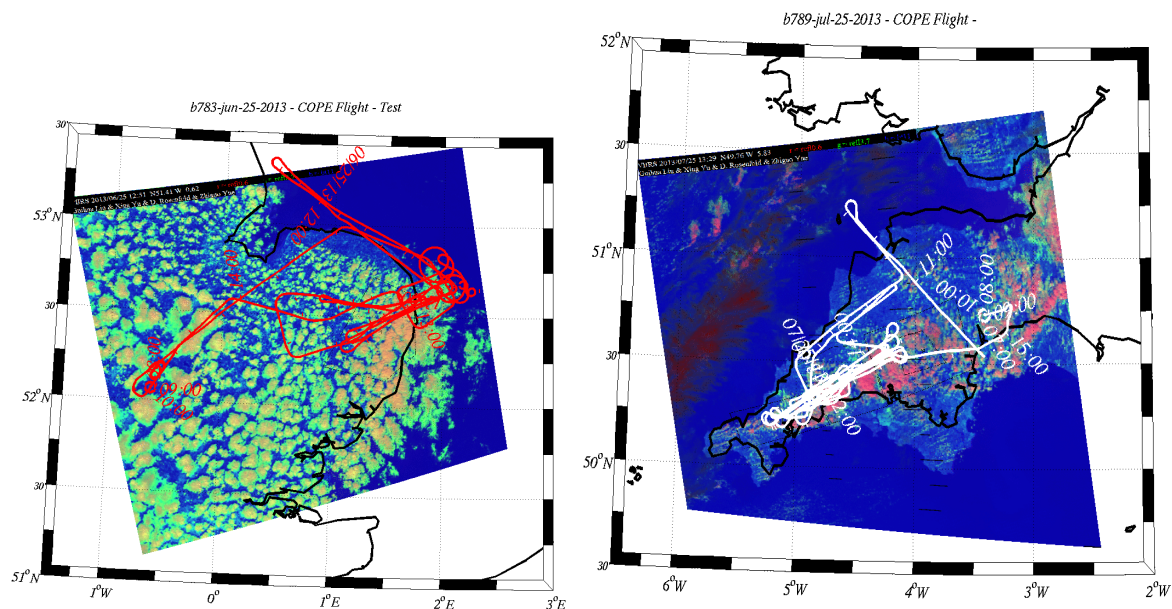


Figure 2. Convective cloud fields sampled with the VIIRS satellite with flight track of aircraft overlaid. Left shows cloud over east anglia on the 25th June 2013; right shows cloud over Cornwall on the 25th July 2013.

The 25th July 2013 case is a clean aerosol case with an active warm rain process. Aerosol size distributions, sampled with the UK's BAe-146 Facility for Atmospheric Airborne Measurements (FAAM) aircraft are shown in Figure 3. These measurements are derived from a Scanning Mobility Particle Sizer (SMPS, $20 < D_p < 600 \text{ nm}$) and a Passive Cavity Aerosol Spectrometer Probe (PCASP, $150 < D_p < 3000 \text{ nm}$). Two measurements are shown for both instruments and these correspond to the coast and inland regions of the study. It can be seen there is very little variation in these size distributions over both regions.

For the bottom-up closure study we fitted three lognormal modes to the aerosol-size distribution, which allows for easy inclusion into parcel models. These are shown in green in Figure 3, with the fit parameters of each mode in the legend. Note that CCN are also measured from the BAe-146 and showed around 280 /cc and 400 /cc at 0.1% and 0.9 % supersaturation respectively. This is consistent with the size distribution measurements in Figure 3.

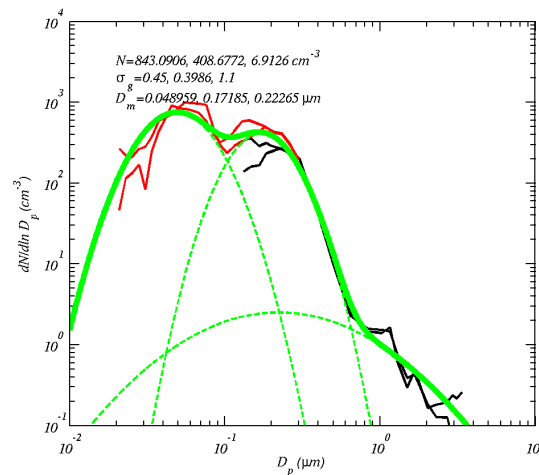


Figure 3. Aerosol size distribution sampled for the COPE case of 25th July 2013. Three lognormal modes have been fitted and the parameters are shown in the legend.

A summary of results from the BAe-146 aircraft and from the Aerosol-Cloud and Precipitation Interactions Model (ACPIM) are shown in Figure 4.

ACPIM is a cloud parcel model developed at the University of Manchester. It is operated as a cloud parcel model here and includes activation / condensational growth (see Topping et al. 2013 and Simpson et al 2014) as well as ice nucleation (Connolly et al. 2009) and collision-coalescence and aggregation (Dearden et al. 2012; Connolly et al. 2012). It is used here to model the activation of cloud drops from observed aerosol particles and their collision and coalescence to form rain. Thus it models the evolution of effective radius within the cloud.

Figure 4a shows the in-cloud vertical wind measurements from the aircraft vs temperature coloured by the liquid water content. In general there is a lot of scatter, but the average is around $0.7\text{-}1.0\text{ m s}^{-1}$. The peaks correspond to turbulence in the rising turrets.

The measurements of effective radius are shown in Figure 4b (black dots). Here we see that the effective radius increases with decreasing temperature at a fairly steady rate; however, at around $0\text{ }^{\circ}\text{C}$, we see a marked change in the rate of increase. This corresponds to the onset of warm rain in the model. The effective radius based on the observed drop concentration (275 cm^{-3}) is shown in red and the maximum values observed are able to reproduce the much of the dependence before the onset of warm rain. The blue dashed line (Figure 4b) is the effective radius calculated from ACPIM; ACPIM is able to capture the onset of warm rain in this case at around $0\text{ }^{\circ}\text{C}$. Green lines are effective radius retrieved from the satellite at different percentiles.

Figure 4c shows the observed cloud drop number concentration (black dots) vs temperature, while the blue dashed line shows the corresponding result from the ACPIM model. Generally the maximum observed values of drop number concentration compare favourably with those from the model. These are assumed to be the convective regions of the cloud.

Figure 4d shows the liquid water content from the observations (black dots) compared to the model (red solid and blue dashed lines). Maxima of liquid water content follow the adiabat, hence, in this case we do observe regions that correspond to adiabatic ascent. We also observe regions with liquid water contents far below adiabatic values so care is needed when making any comparisons.

For this case, looking at the cloud properties at $0\text{ }^{\circ}\text{C}$, we can see from the satellite that the effective radius is $20\text{ }\mu\text{m}$ and the liquid water content is around 3 g m^{-3} . Hence, applying Equation 1, we retrieve that the drop concentration is $\sim 100\text{ cm}^{-3}$. However, we see in Figure 4b that the measured drop concentration is around a factor of 2 higher than this - approximately 350 cm^{-3} .

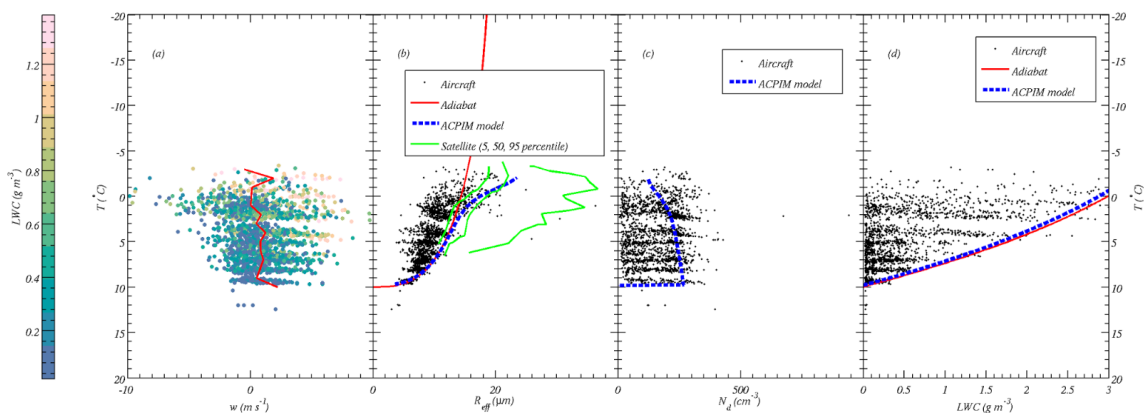


Figure 4. Comparison of in situ observations sampled during the COPE flight of the 25th July 2013 with simulations from the ACPIM parcel model. (a) shows the in-cloud vertical wind; (b) shows the effective diameter sampled with cloud, modelled and retrieved by satellite; (c) shows the cloud drop number concentration; (d) shows the liquid water content.

Inverse Parcel Modelling

The cumulus congestus case has been used as a basis to develop an inverse parcel modelling framework based on coupling a Markov Chain Monte Carlo (MCMC) algorithm to a pseudo-adiabatic cloud parcel model, following the methodology presented in Partridge et al., (2012).

Here aerosol and meteorological input parameters are taken from the case study data above, along with their associated parameter uncertainty. This uncertainty is probed via the MCMC algorithm, which randomly generates parameter values across the multi-dimensional parameter space, these values are then used to initiate the cloud parcel model to explore the dependence of the simulated model output (profiles of droplet effective radius) on perturbations to the input parameters via the computation of a likelihood function (typically defined similar to the RMSE). This likelihood function provides a diagnostic measure of how well the model fits the data. It essentially measures the distance between the model predictions and corresponding observations (see Partridge et al., 2011).

The framework aims to converge on the observations (mean and error), which in this case is the profile of effective radius. Initially, this framework has been applied to a cloud parcel model with only the process of droplet activation considered; hence, it is unable to model the observed sharp increase in effective radius around 2 °C. Now that the framework has been successfully tested, these simulations will be repeated with the process of collision-coalescence turned on. Nevertheless, it does allow some useful insight.

Figure 5 illustrates the observations of effective radius (green line) in addition to several model realisations of effective radius (grey lines) that correspond to random perturbations of the input parameter space, and the ‘best’ solution (blue line). The MCMC model framework converges on the solutions that best match the observation data. This allows us to assess the sensitivity to different input parameters.

We have assessed the sensitivity of the computations to the properties of the aerosol input distribution (number concentration, width parameter and median diameter, shown in the legend of Figure 4) as well as the vertical wind speed. The range of inputs (prior range) probed is given in Table 2.

Table 2. Prior range of values for MCMC method. True values are the best point estimates, whereas max and min are the considered ranges.

	Max	Min	True values
$N_a(\text{cm}^{-3})$	470.35	347.65	409
$\ln \sigma_g$	1.71	1.27	172
$D_m(\text{nm})$	197.8	146.2	1.49
$w (\text{m s}^{-1})$	1.30	0.10	0.7

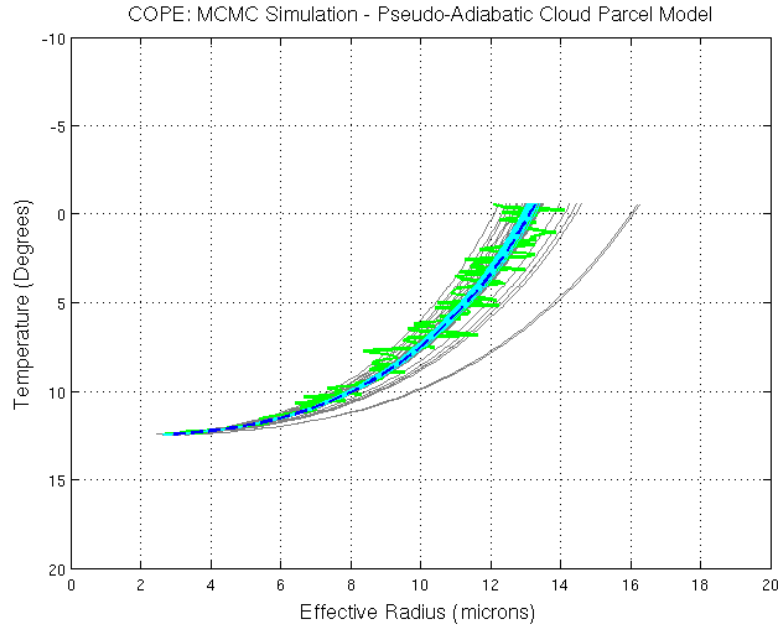


Figure 5. Illustrating successful convergence of parcel model to a synthetic observation of effective radius. Green is the observation data; grey are several model solutions for different inputs over the prior input parameter distribution and blue dotted line is the best solution and cyan lines are model solutions corresponding to the posterior input parameter distribution.

The output of the MCMC framework, driven by the parcel model, is shown in Figure 6. Figure 6 illustrates the convergence of input parameters from our input range (the prior distribution) to the range of values that best match the observations (the posterior distribution). In each panel, each colour corresponds to a separate Markov chain that is exploring the multi-dimensional parameter space. For instance, the green dots in each panel of Figure 6 correspond to the same Markov chain (see Partridge et al. 2012). We can see Figure 6 (top left, top right, bottom left panels) that the posterior distribution (the values after convergence to the limiting distribution that results in a good fit to the effective radius profile observations) of particle concentrations, radius and geometric standard deviation are distributed evenly over the prior range of inputs.

However, in Figure 6 (bottom right panel) we can see that the updraft parameter converges to a narrower distribution (as the iteration number increases). This tells us that the updraft has to be in the range 0.55-0.9 in order to match the observations. On the other hand the other parameters can be any value given the provided range and we are still able to match the observations -thus, for this model the observations of the effective radius profile are insensitive to their perturbations across the prior range explored

The implications here are that, to within measurement uncertainty, we can find closure between the observed aerosol and cloud properties for this case; hence, the approach can help us narrow down the uncertainty in the updraft speed. It also suggests that cloud base updrafts need to be well constrained to derive CCN from the observed effective radius profiles. This may not be the case for deeper convection.

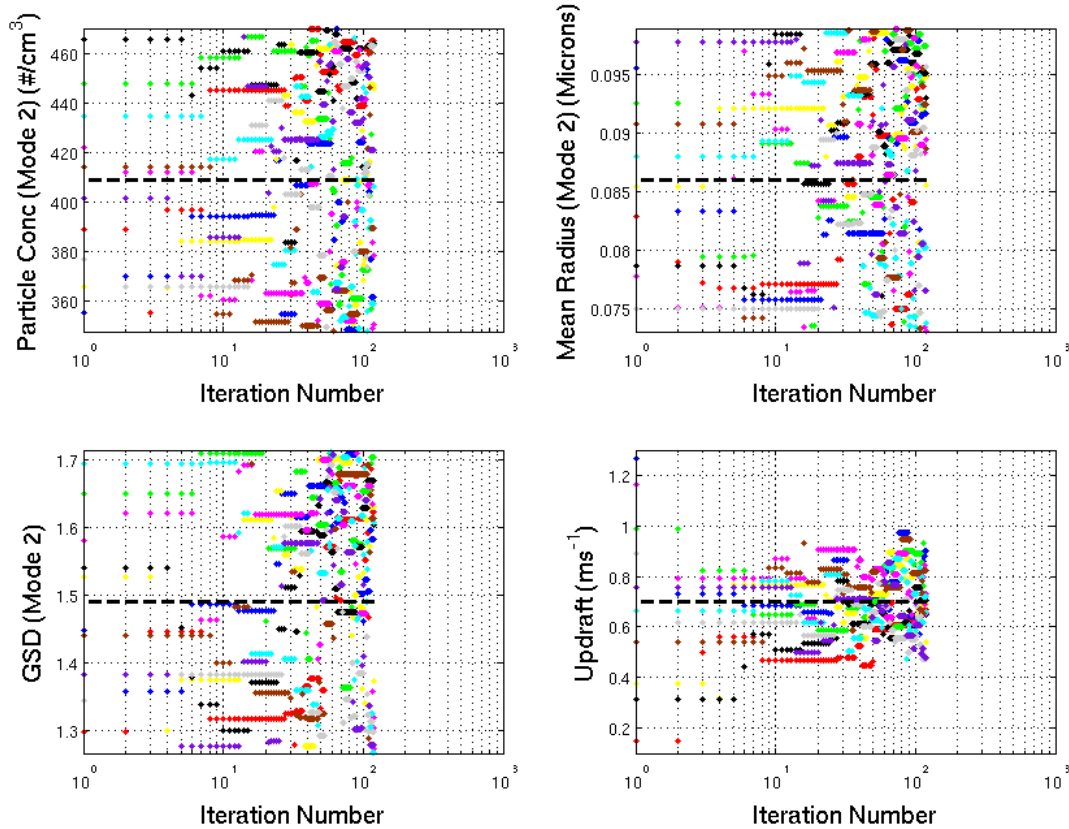


Figure 6. Values of particle concentration, mean radius and geometric standard deviation as well as updraft velocity (displayed on the y-axis) that the MCMC algorithm chooses as it converges on a solution that best matches the observations. The only parameter converging in this case is the updraft speed.

Convective Cloud Field Model

The Convective Field Model (CCFM, Wagner and Graf, 2010) is a spectral parametrization of convection, used in the GCM ECHAM-HAM. It simulates a population of entraining plumes, having different cloud base radius and vertical velocity. This allows for different cloud drop number concentration in each cloud type. To compare with satellite measurements we use the CCFM in a single column model (SCM) setup. The required forcing dataset from variational analysis of radiosonde data is only available for the GOAMAZON campaign. Work on improving the CCFM cloud microphysics is ongoing in BACCHUS: here, we have used the standard single-moment microphysics (Zhang et al. 2005) where cloud drop number concentration is calculated at cloud base using the ARG activation scheme (Abdul-Razzak and Ghan 2000). The average drop radius is then calculated using the modeled cloud liquid mass mixing ratio and drop number concentration. Initial results are shown in Figure 7.

Here it can be seen that, at least for this case, the single-moment microphysics of this version of CCFM struggles to reproduce the effective radius dependence on cloud temperature; the

decrease in modeled droplet radius is related to the formation of rain and ice and the assumption of a constant number of cloud droplets in the parcel. Further improvements to the microphysical representation are underway to address these issues. The results suggest that a true two-moment representation is necessary to model the the vertical profile of the cloud effective diameter. Other factors may contribute to the difference with the observations: the satellite retrievals are done within a polygon of fairly limited spatial dimensions while CCFM cloud spectrum is representative of convection over a much larger GCM gridbox (about 200 km x 200 km), so that we will have to investigate possible selection bias and representativity issues.

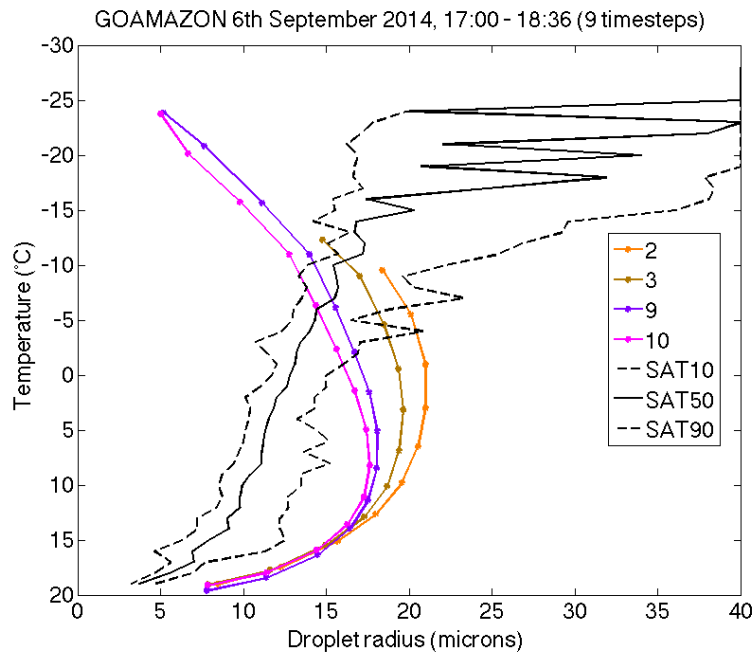


Figure 7. Comparison of drop radius from CCFM (for the cloud types 2, 3, 9 and 10 of the simulated cloud spectrum, that were the only one present during the period) against the available satellite retrievals(10, 50 and 90th percentile).

Findings and recommendations

Our results suggest ways forward to improve the retrieval of cloud drop number concentration from the NPP / VIRRS satellite instrument. The shallow clean cases over the UK show that cloud drop effective radius is in fair agreement with in-situ observations and this can be modelled with a drop activation / collision-coalescence model; however, the cloud drop number concentration seems to be underestimated. We believe this is because of the broadness of the drop distribution in cloud over the UK and its effect on the effective radius (e.g. similar to the ideas of Liu and Daum, 1999).

Figure 8. shows a plot of the size distribution observed on the BAe-146 aircraft, as measured with the Droplet Measurement Technologies (DMT) Cloud Droplet Probe (CDP) and the SPEC Inv

2D-Stereographic Probe (2DS). It is evident that the size distribution is quite broad, so the assumption of using the effective radius to calculate the liquid water content may not hold.

We can improve on this to a first order by assuming an exponential distribution for the cloud drops:

$$n(r) = n_0 \exp(-\lambda r)$$

where n_0 is the intercept parameter and λ is the slope parameter

In this case we can define the effective radius as (the ratio of 3rd and 2nd moments)

$$r_{eff} = \frac{3}{\lambda}$$

The total cloud drop number concentration is

$$N_d = \frac{n_0}{\lambda}$$

and the liquid water content is

$$LWC = \frac{8\pi\rho n_0}{\lambda^4}$$

Hence, if we know N_d and LWC we can eliminate n_0 and find λ :

$$\lambda = \left(\frac{8\pi\rho N_d}{LWC} \right)^{1/3}$$

This is inserted in r_{eff}

$$r_{eff} = \left(\frac{27LWC}{8\pi\rho N_d} \right)^{1/3}$$

we can thus calculate the drop number by rearranging:

$$N_d = \frac{27LWC}{8\pi\rho r_{eff}^3}$$

Using the observed values from the case study (LWC=3 g m⁻³ and r_{eff} =20 μm we calculate that the drop concentration is 400 cm⁻³. While this is not perfect agreement it does demonstrate that the assumed shape of the distribution is important to the retrieval.

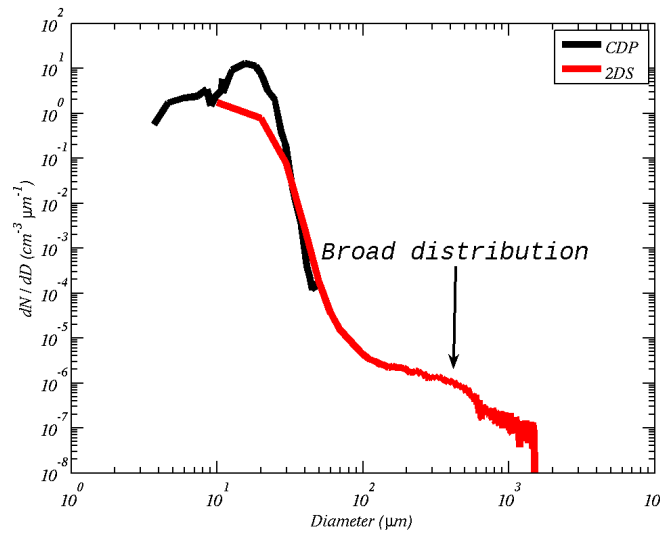


Figure 8. A size distribution from the COPE case on 25th July 2013. It shows the need to represent the larger drops in the effective radius retrievals.

Changes with respect to the DoW

In this task we have combined traditional bottom-up CDNC/ICNC closure studies with a novel concept of top-down closures studies to provide constraints on the satellite inferred cloud microphysical properties concentrations. Our initial work focused on the development of the methodologies, demonstrating the feasibility of this concept and the application to a limited number of case studies. In current and future work we will extend our methodologies to additional BACCHUS case studies (Table 1) to cover a wide range of cloud regimes. Initially, this work will focus on cases of deep convection over the Amazon. For example, Figure 9 shows a case from the SAMBBA field campaign, which will be developed further.

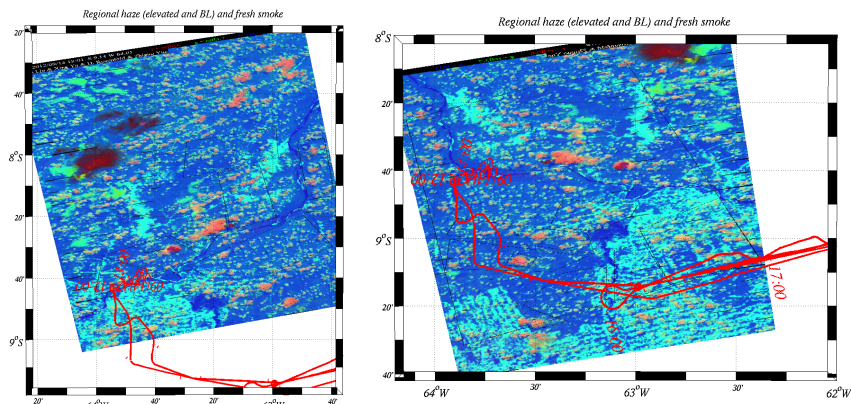


Figure 9. Two images from NPP / VIIRS with overlaid flight track from the SAMBBA campaign showing the path of the aircraft through the clouds. Left is image to the north and right to the south. Flight track is the same in both cases.

In addition, the GO-AMAZON case study is the only dataset with variational analyses of forcing fields required to run MPI-ESM-CCFM in single column mode. Additionally, the University of Munich retrieved profiles of cloud droplet effective radii using an airborne side scanning instrument that would provide an additional independent constraint. Unfortunately, data from this campaign is not yet widely available as the project only took place 1 year ago. We are in contact with a number of data PIs to secure early access to this very comprehensive dataset.

Dissemination and uptake

Within the project, this work provides direct input to:

1. The retrieval of cloud droplet numbers and CCN from satellites in WP1 (T1.5)
2. The ongoing case studies to investigate the key processes controlling cloud systems in contrasting environments process studies in WP3 (T3.2)
3. The evaluation of CCFM directly feeds into the Evaluation of global ESMs (T3.4)

Outside of the project we expect our results to make impact by:

1. Demonstrating the feasibility of this new combined bottom-up / top-down closure study framework
2. Influencing the retrieval of droplet numbers and CCN from satellite based instruments
3. Close cooperation with key external partners, e.g. the work on MCMC parcel modelling has been conducted in close cooperation with Dr Daniel Partridge from the University of Stockholm.
4. Improving the representation of convection in current and future ESMs, as demonstrated by the evaluation of MPI-ESM-CCFM in this work.

References

- ❑ Abdul-Razzak, H., and Ghan, S. J. : A parameterization of aerosol activation: 2. Multiple aerosol types, *J. Geophys. Res.*, 105(D5), 6837–6844, doi:10.1029/1999JD901161., 2000
- ❑ Connolly, P. J., O. Möhler, P. R. Field, H. Saathoff, R. Burgess, T. Choularton, and M. Gallagher Studies of heterogeneous freezing by three different desert dust samples *Atmos. Chem. Phys.*, 9, 2805-2824, 2009
- ❑ Connolly, P. J., C. Emersic, and P. R. Field A laboratory investigation into the aggregation efficiency of small ice crystals *Atmos. Chem. Phys.*, 12, 2055-2076, 2012
- ❑ Dearden, C., P. J. Connolly, T. Choularton, P. R. Field and A. J. Heymsfield Factors influencing ice formation and growth in simulations of a mixed-phase wave cloud *J. Advances in Modelling Earth Systems*, 2012, DOI: 10.1029/2012MS000163

- ❑ Freud E., D. Rosenfeld, and J. R. Kulkarni, Resolving both entrainment-mixing and number of activated CCN in deep convective clouds, *Atmos. Chem. Phys.*, 11, 12887-12900, 2011
- ❑ Liu Y. and Daum P. H. Spectral dispersion of cloud droplet size distributions and the parameterization of cloud droplet effective radius. [Geophysical Research Letters](#). 07/2000; 27(13):1903-1906. DOI: 10.1029/1999GL011011
- ❑ Partridge, D. G., Vrugt, J. A., Tunved, P., Ekman, A. M. L., Gorea, D., and Sorooshian, A.: Inverse modeling of cloud-aerosol interactions – Part 1: Detailed response surface analysis, *Atmos. Chem. Phys.*, 11, 7269-7287, doi:10.5194/acp-11-7269-2011, 2011.
- ❑ Partridge, D. G., Vrugt, J. A., Tunved, P., Ekman, A. M. L., Struthers, H., and Sorooshian, A.: Inverse modelling of cloud-aerosol interactions – Part 2: Sensitivity tests on liquid phase clouds using a Markov chain Monte Carlo based simulation approach, *Atmos. Chem. Phys.*, 12, 2823-2847, doi:10.5194/acp-12-2823-2012, 2012.
- ❑ Rosenfeld, D., E. Williams, M. O. Andreae, E. Freud, U. Pöschl, and N. O. Rennó, The scientific basis for a satellite mission to retrieve CCN concentrations and their impacts on convective clouds, *Atmos. Meas. Tech.*, 5, 2039–2055, 2012.
- ❑ Simpson, E. P. Connolly, and G. McFiggans An investigation into the performance of four cloud droplet activation parameterisations *Geosci. Model Dev.*, 7, 1535-1542, 2014
- ❑ Topping D., Connolly P & McFiggans G. Cloud droplet number enhanced by co-condensation of organic vapours *Nature Geoscience* 6, 443–446 (2013) doi:10.1038/ngeo1809
- ❑ Wagner, T. M., and Graf, H.-F.: An Ensemble Cumulus Convection Parameterization with Explicit Cloud Treatment, *J. Atmos. Sci.*, 67(12), 3854–3869, doi:10.1175/2010JAS3485.1., 2010
- ❑ Zhang, J., Lohmann, U., and Stier, P.: A microphysical parameterization for convective clouds in the ECHAM5 climate model: Single-column model results evaluated at the Oklahoma Atmospheric Radiation Measurement Program site, *J. Geophys. Res.*, 110(D15), D15S07, doi:10.1029/2004JD005128., 2005